NANO LETTERS

2007
Vol. 7, No. 9
2676−2683

Robust Inorganic Membranes from Detachable Ultrathin Tantalum Oxide Films

Sherdeep Singh, Mark T. Greiner, and Peter Kruse*

Department of Chemistry, McMaster University, 1280 Main Street West, Hamilton, Ontario L8S 4M1, Canada

Received May 6, 2007; Revised Manuscript Received July 17, 2007

ABSTRACT

We report a simple electrochemical method of making individual free-standing and uniform tantalum oxide membranes between 35 and 100 nm thick. These films can be separated, floated on water, and transferred onto various substrates such as Si wafers, glass slides, and TEM grids. Our membranes are mechanically, chemically, and thermally robust, have a high dielectric constant, and a high refractive index, making them potentially useful in sensors, optics, filtration, and catalysis.

Tantalum metal was discovered in 1802 by Anders Gustav Ekeberg,[1] who named it after the mythological Greek figure Tantalus, whom the gods condemned to endure thirst while standing in a pool of water. Ekeberg found the chemical inertness of tantalum toward aqueous acids to be analogous to Tantalus' inability to drink from the water. The origin of this inertness is a thin protective layer of tantalum oxide (Ta_2O_5) at the metal surface. Consequently, tantalum and its oxide have found applications in chemical reactors, airplanes, and corrosion protection coatings for biomedical implants, surgical instruments,[2,3] and sensors.[4]

Tantalum oxide possesses several other remarkable properties. For example, Ta_2O_5 and its composites exhibit photocatalytic activity and have been used as catalytic substrates for the photolysis of water to yield molecular hydrogen and oxygen, a reaction that can be used to harness solar energy.[5,6] Tantalum oxide also has a very high refractive index and is being used in antireflective coatings for lenses and solar panels.[7] As a piezoelectric material, it can be used in surface acoustic wave devices[8] such as band-pass filters and various types of mechanical sensors. Because of their very high dielectric constant and good compatibility with silicon, thin films of tantalum oxide are also used in thin film transistors,[9,10] ion-sensors,[11] and storage capacitors for dynamic random access memory.[12−14] Recently, thin sheets of metal oxides have found use as dielectric spacers between metal electrodes for fabricating negative refractive index materials, also known as metamaterials.[15,16] These properties have resulted in increased interest in these films and their fabrication.

High quality compact films of tantalum oxide with well-defined thickness can be grown by anodization in a variety of electrolytes.[17,18] Dilute aqueous solutions of hydrofluoric acid, however, result in porous films due to partial dissolution of the formed oxide, with the degree of porosity depending on the fluoride ion concentration.[19] Hydrofluoric acid is the only chemical capable of attacking tantalum oxide. If tantalum is anodized in nonaqueous solutions of hydrofluoric acid, all oxide is dissolved immediately as it is formed, resulting in an electropolished tantalum surface instead of an oxide film. The fast dissolution can be attributed to the poor quality of the oxide due to high levels of incorporation of electrolyte ions.[20,21] For example, tantalum can be electropolished in a mixture of H_2SO_4 (95−98%) and HF (48%) in a 9:1 volumetric ratio.[10,20−22] The resulting flat surface is well-suited to the growth of anodic oxide films.[10]

If a Ta_2O_5 film is desired on a substrate other than tantalum itself, a different approach such as reactive sputtering (SP),[23,24] reactive ion plating (IP),[25] pulsed laser-assisted evaporation, or chemical vapor deposition (CVD)[26−28] is required. These techniques are well established on hard substrates but are limited by substrate damage during thin film growth, lack of vacuum compatibility in the case of soft or biological substrates, contamination due to silicon migration at elevated temperatures, and carbon deposits from organometallic precursors. Thin films grown by these techniques are static and cannot be transferred onto other substrate surfaces or used free-standing, which is desirable for applications as sheet actuators, organized catalyst surfaces, nanolithographic templates, and separation membranes. For other materials, this limitation has recently been over-

* Corresponding author. E-mail: pkruse@mcmaster.ca. Telephone: (905) 525-9140 x23480. Fax: (905) 522-2509.

10.1021/nl071061z CCC: $37.00
Published on Web 07/31/2007

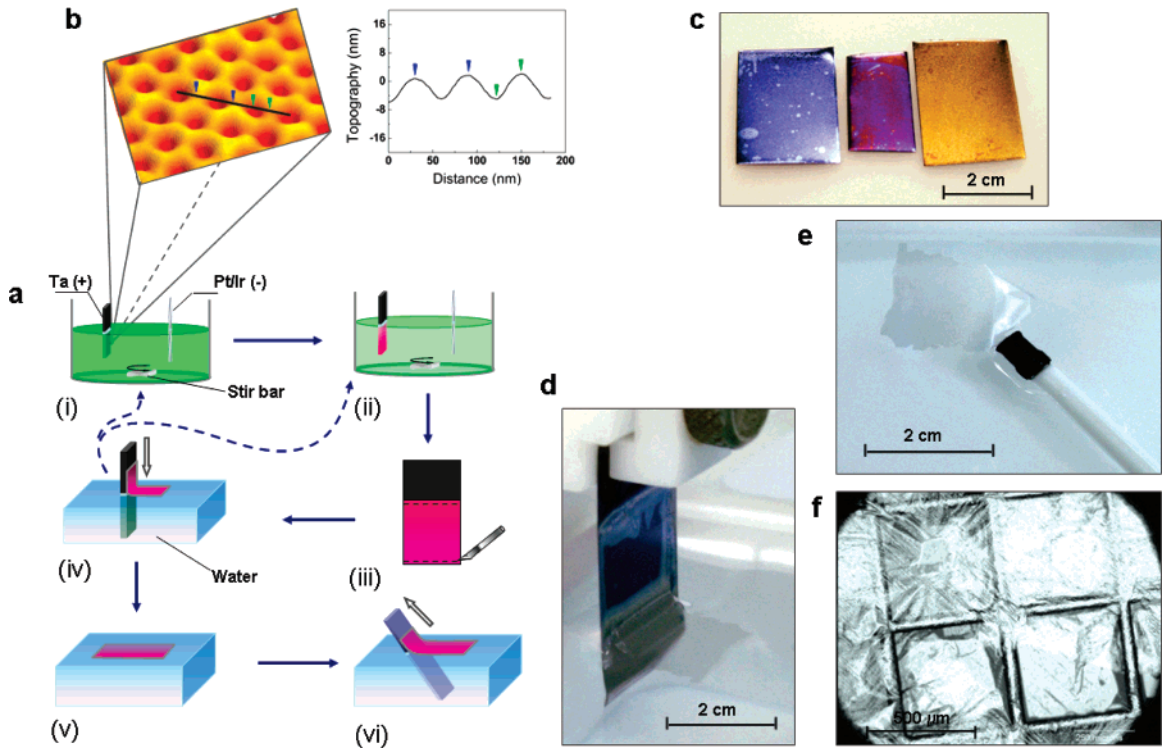

Figure 1. Scheme for fabricating tantalum oxide membranes. (a) Electropolishing of the tantalum surface (i); anodic growth of the oxide film (ii); scratching of oxide film at the borders to facilitate detachment (iii); detachment of the film at the air−water interface (iv); film floating on water (v); transfer of the film onto a substrate (vi). (b) AFM image with cross section showing the formation of dimples due to electropolishing. (c) Photographic image showing colors corresponding to different oxide thickness (from left to right: 5, 3, and 1 min growth time). (d) Photographic image of the detachment process. (e) Photographic image showing an oxide film floating on water after complete detachment. (f) Free-standing tantalum oxide membrane after transfer onto a TEM grid.

come by the synthesis of free-standing organic−inorganic hybrid sheets.[29−32]

Here we report a simple and inexpensive, solution-based method for producing transferable, robust, and purely inorganic membranes of Ta_2O_5. They are chemically more inert and thermally more stable than composite organic−inorganic membranes and mechanically superior to previously reported inorganic membranes such as porous alumina. We have fabricated and transferred uniform films as large as 2 cm by 3 cm, limited by the size of our equipment. Tantalum oxide films with a controlled thickness of as little as 35 nm and up to more than 100 nm are first grown on tantalum foil and then separated as sheets by the lift-off-float-on (LOFO) technique. These sheets can be used as free-standing membranes or transferred from the air−water interface to a wide variety of substrates such as Si wafers, glass slides, and TEM grids. Despite the extreme aspect ratio, these sheets remain intact throughout the transfer process. Their morphology can be tuned from ordered mesoscale dimples to nanosized pores by adjusting the anodizing parameters such as voltage and composition of the electrolyte solution.

To fabricate large, uniform oxide sheets from commercially available cold-rolled tantalum foil (Alfa Aesar, 99.95%, 0.127 mm), it is first necessary to electropolish the surface (Figure 1a(i)). This is achieved by anodizing the tantalum foil at 15 V in a 9:1 volumetric mixture of concentrated sulfuric acid (95−98%, Fisher Scientific, reagent grade) and concentrated hydrofluoric acid (48%, Fisher Scientific, semiconductor grade; see ref 22 for further details). We have previously reported that electropolishing of a tantalum surface under these conditions generates highly ordered dimples at the nanoscale (Figure 1b), 30−50 nm in diameter and around 8−10 nm deep.[22] The oxide layer on the tantalum surface at this stage is equivalent to the native oxide that forms on tantalum in air.

In the second step, the tantalum oxide films are grown on electropolished (dimpled) tantalum samples by anodizing them in an aqueous electrolyte containing 1M H_2SO_4 and 2 wt % HF at constant voltage of 20 V (Figure 1a(ii)). Fluoride ions are required to weaken the adhesion of the anodic film to the underlying metal so that the film can be peeled off. Even a low concentration of fluoride ions (0.1 wt % HF in 1M H_2SO_4) is sufficient for the detachment of oxide sheets, however, the fluoride ion concentration affects the pore size. Because of interference of light, the films exhibit brilliant photonic colors (Figure 1c) that depend on their thickness, i.e., the anodization time. The thickness of the films can be estimated in situ by observing their color change during anodic oxidation. The colors of these films can also change, depending on whether they are wet or dry, due to a change in refractive index when the porous films are soaked with solvent. This property can be utilized in Bragg reflector sensors for the detection of various chemicals and biologically relevant molecules. Sensors of this type have

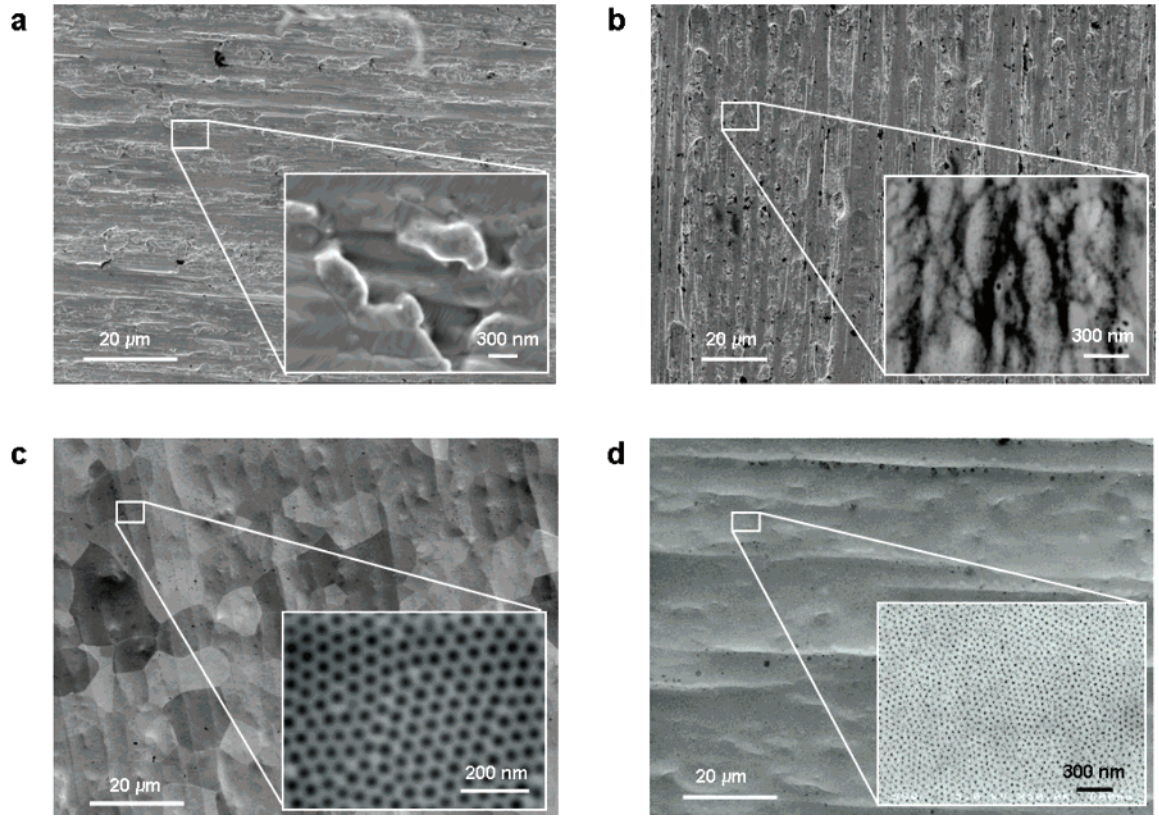

Figure 2. SEM images demonstrating the importance of electropolishing the tantalum surface before oxide film growth. (a) As-received cold-rolled tantalum sample surface. (b) Porous oxide film grown directly on a cold-rolled tantalum sample. (c) Tantalum surface after electropolishing, exhibiting characteristic dimples. (d) Porous oxide film grown for 5 min in 2 wt % HF on an electropolished sample, showing the high quality of the films with pores that loosely align themselves with the dimples from electropolishing.

already been demonstrated based on other porous oxide films and butterfly wings.[33−36]

Under the conditions described above, the films can be completely detached as large, continuous sheets using the LOFO technique. Because wet films are easier to detach than dry films, the tantalum oxide samples are rinsed with deionized water before detachment. The upper and lower edges of the oxide film are then scratched with a needle to facilitate its detachment (Figure 1a(iii)). The lower scratch allows the penetration of water under the tantalum oxide film for lifting it from the tantalum surface. A small bend near the lower edge also helps to initiate film detachment. The upper scratch makes a well-defined boundary for the film. If an appropriately scratched sample is slowly immersed (8 mm/min) into water using the dipper of a Langmuir−Blodgett trough (KSV-2000, KSV Instruments Ltd.), the film will separate (Figure 1a(iv),d). The separated films float as large sheets on the water surface (Figure 1a(v),e). These sheets can then be transferred onto glass or silicon substrates by slowly pulling the substrate up from underneath the floating film (Figure 1a(vi)). Alternatively, the films can be transferred onto a supporting mesh such as a TEM grid (Figure 1f).

The ease of oxide film detachment as described in our process is somewhat surprising because compact Ta_2O_5 films are generally known to be well-controlled, with few defects and highly adherent to the underlying tantalum metal.[17,18] Even thick compact oxide films grown on dimpled surfaces have been reported to not detach.[10] We will show that the presence of fluoride ions during the anodic oxide growth step is crucial for detachment. However, the presence of fluoride ions during porous oxide growth on tantalum as reported previously by Schmuki et al.[19] is not sufficient to prepare high quality oxide films for detachment if the surface is not first electropolished. The electropolishing step is required to remove the macroscopic surface roughness of the as-received tantalum foil (Figure 2a) because the roughness exceeds the oxide film thickness (Figure 2b), leading to the separation of small, nonuniform pieces during film transfer. The electropolishing of tantalum generates a clear grain structure with a pattern of wavy lines remaining on the surface (Figure 2c), which are artifacts of the cold-rolling process used to manufacture the tantalum foil. Even though these lines are imprinted onto the tantalum oxide films (Figure 2d), they do not present a problem in the fabrication of the membranes.

Detachment of the films becomes gradually more difficult as the thickness of the oxide layer increases. The most easily separable films are obtained by growing the oxide for no longer than 10 min in a 1M H_2SO_4, 2 wt % HF solution at 20 V. Peeling of an oxide film grown for 5 min under these conditions leaves a clean surface of the pure tantalum substrate covered with native oxide (Figure 3a). In contrast, anodic oxide films grown for 15 min or more are very difficult to detach. The texture of the surface beneath the films also changes with increasing thickness of the films.

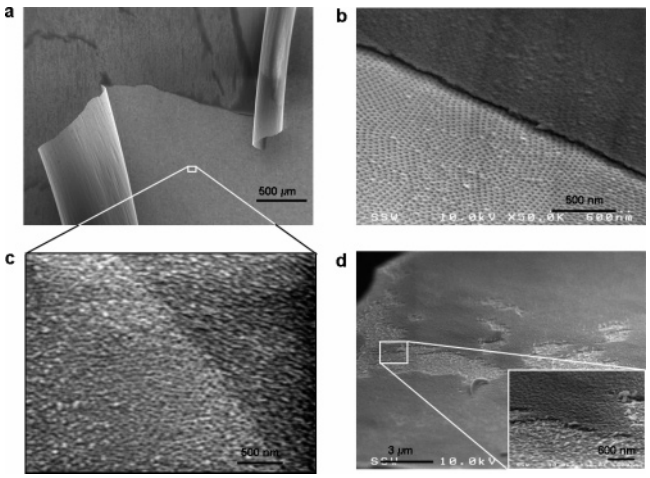

Figure 3. SEM images of the film peeling process. (a) Partially detached and rolled-back oxide film on the tantalum surface. (b) Boundary of an oxide film after 1 min of oxide growth on a dimpled surface, showing dimples both on the remaining oxide film and on the freshly peeled surface. (c) Irregular structure of a surface left behind after peeling a film that was grown for 5 min on a dimpled surface (close-up from area of panel a). (d) Remnant interfacial oxide after detachment of a film that was grown for 10 min on a dimpled surface.

The underlying tantalum surface shows a shallower dimpled morphology after peeling of a 35 nm thick film formed after anodizing for 1 min in (1M H_2SO_4, 2 wt % HF) solution (Figure 3b). The texture of surface left behind by a 5 min film (Figure 3c) differs in morphology: no ordered dimples are discernible despite a comparable overall feature size and smoothness. This substrate can be used to make further flat tantalum oxide films without the dimpled morphology. Alternatively, the electropolishing step can be repeated at this point to regenerate the dimples. We peeled off four films (5 min oxide growth) in sequence from the same sample using this method, but there is no obvious limit to the number of detachable films other than the thickness of the tantalum substrate.

Oxide films grown for 10 min (1M H_2SO_4, 2 wt % HF, 20 V) leave undetached flakes of oxide (a few nm thick) behind on the surface, but the film still peels off uniformly (Figure 3d). The amount of oxide left on the surface after peeling off the films is measured with nuclear reaction analysis (NRA) using the $^{16}O(d,p)^{17}O$ nuclear reaction with a 972 keV deuterium primary beam (1 mm^2). NRA reliably gives a signal that is strictly proportional to the total oxygen content in the near surface region (approximately 0.5 μm deep) of the sample. A compact Ta_2O_5 film of a known thickness of 70.7 nm serves as a calibration standard. More about the experimental setup of the NRA system at Interface Science Western can be found elsewhere.[37] The average thickness (over 1 mm^2) of the oxide remaining on the tantalum surface after peeling increases from 2.1 and 2.2 nm for the 1 and 5 min samples, respectively, to 3.1 nm for the 10 min sample. Clearly, the structure of the films changes with time during the oxide growth process.

A closer look at the cross section of a 5 min film (Figure 4a) reveals the heterogeneous structure. A very porous layer rests on a more compact looking oxide with a narrow stripe (dark in Figure 4a) at the interface to the tantalum metal that likely plays a role in detachment. The evolution of tantalum oxide films during anodic oxidation in F^- containing solutions has been studied before.[38,39] It was shown that the anodization current during oxide growth is mainly related to the migration of ionic species (F^-, O^{2-}, OH^-) from the electrolyte toward the metal−metal oxide interface and Ta^{5+} from the metal toward the oxide−electrolyte interface under the applied potential. The higher mobility of F^- as compared to O^{2-} was shown to result in a thin tantalum fluoride rich layer at the metal−metal oxide interface. We performed depth profiling time-of-flight secondary ion mass spectrometry (TOF−SIMS) on our films to analyze the changes in film chemistry under our specific conditions. Because the $^{16}O^-$ and $^{19}F^-$ channels were saturated during part of the depth profile (see Supporting Information), we followed $^{18}O^-$ and $^{19}F_2^-$ instead. Sulfate was followed as $^{32}S^{16}O^-$, tantalum oxide is represented in Figure 4 as $^{181}Ta^{16}O^-$, and tantalum fluoride and oxyfluoride as $^{181}Ta^{19}F^-$. The results are consistent with literature reports,[38] but for the first time also illustrate the transition between detachable and nondetachable films.

The depth profile of the 1 min sample (Figure 4b) shows a very pronounced spike in the fluoride concentration at the interface between tantalum oxide and tantalum. This is a sign of an interfacial layer rich in tantalum oxyfluoride and tantalum fluoride species, which are soluble in water, leading to the very facile detachment of the film. This picture changes for the 10 min sample (Figure 4c, characteristic mass spectra provided in the Supporting Information), where the fluorine peak has broadened and become shallower. Indeed, films from 10 min samples (e.g., Figure 3d) do not detach as easily. While tantalum fluoride and oxyfluoride continue to be present in the film, they are dispersed in an insoluble tantalum oxide matrix. Finally, a 20 min sample (Figure 4d) no longer has an interfacial layer with elevated fluoride concentration even though a spike in sulfate concentration is visible in the center of the film, possibly associated with the bottom of the highly porous top layer. Fluoride and oxyfluoride species are present throughout the film, but the insoluble tantalum oxide matrix now firmly holds the anodic film on the tantalum surface.

The lack of a distinct fluoride peak at the metal−oxide interface in the case of longer oxide growth times is not consistent with earlier findings[38] that the migration speed of fluoride ions within the films exceeds that of oxide ions. We note that even though those findings concern thicker oxide films than reported here, Shimizu et al. also employed considerably higher anodization voltages (100V) than in our study (20 V). Irrespective of voltage, high concentrations of fluoride ions get incorporated into the films during the initial stages of oxide film formation. Initially, fluoride ions migrate faster than oxide ions, thus keeping up with oxide film growth. However, as the field gradient within the film decreases below a critical value of about $^1/_3$ V per nm due

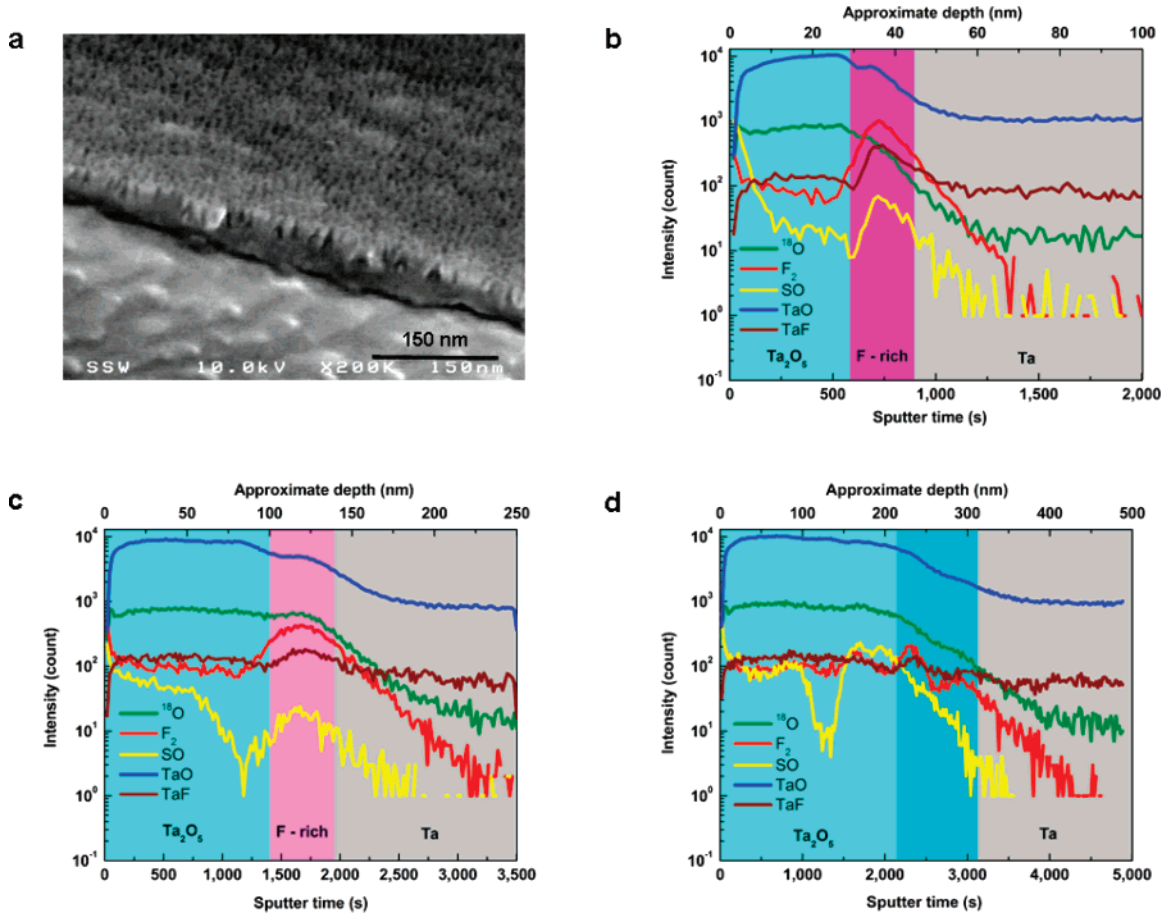

Figure 4. SEM micrograph of cross-sectional structure and ToF-SIMS depth profiling data of tantalum oxide films grown for different times. (a) Close-up of the edge of a partially detached 5 min oxide film. (b) Depth profile of a film grown for 1 min. (c) Depth profile of a film grown for 10 min. (d) Depth profile of a film grown for 20 min.

to the increase in film thickness, fluoride ions fall behind oxide ion migration as evidenced by the data presented in Figure 4.

The detachment of films from the tantalum surface at the air−water interface can be understood by considering the surface forces and the dissolution of tantalum fluoride in water. Penetration of water between the metal and the metal oxide film initiates the film detachment. The film detaches due to the interfacial forces at the triple contact line (air−water−substrate) and simultaneous dissolution of tantalum fluoride. We were not successful in detaching these films using low surface tension liquids such as acetone and ethanol even when they were first rinsed in water. Using a Wilhelmy plate, the surface tensions of water, acetone, and ethanol are measured to be 72 mNm^{--1}, 23 mNm^{-1}, and 22 mNm^{-1}, which compares well with literature values of 73.05 mNm^{-1} at 18 °C, 23.70 mNm^{-1} at 20 °C, and 22.75 mNm^{-1} at 20 °C, respectively.[40] Lack of solubility of tantalum fluoride in acetone and ethanol may be a contributing factor, however, we note that the wetted films can be easily and completely peeled off using scotch tape. A subphase with higher surface tension (such as water) assists the detachment process, as has been reported before by Vilan et al.[41] during the separation of thin metal films from a variety of substrates. Nevertheless, it was observed that the films can float on low surface tension liquids like acetone and methanol by slowly exchanging the water underneath the films with these liquids. It should also be noted here that ultrasonication in water for 20 to 30 s is an alternative way of detaching the oxide films as small shards of a few square millimeters in size.

The uniform separation and transfer of large membranes illustrate their high mechanical strength. They can even roll and bend, showing a certain degree of flexibility (Figure 3a). Previous studies[42,43] of the mechanical properties of tantalum oxide films show that porous tantalum oxide films are much more ductile (Young's modulus of 140 ± 14 GPa) than porous alumina films and can withstand up to 50% deformation before fracture. The tantalum oxide membranes reported here are stronger, thinner, and have smaller size pores than porous aluminum oxide membranes, which are used as templates in a large number of applications.[44,45]

The sheets are uniform and flat over large areas and can contain ordered arrays of dimples 30−50 nm in diameter that are riddled with small pores perpendicular to the metal−metal oxide film interface (Figure 5). The porosity arises from the dissolution of Ta_2O_5 by HF. The effect of fluoride ion concentration in the electrolyte solution is shown in Figure 5a−c. The pore density and pore size increase as the HF concentration increases from 0.5 wt % to 4 wt % in 1M H_2SO_4 solution. It is also observed that the pores in films grown on dimpled tantalum sheets (Figure 5 b,c) are slightly more ordered than pores in films grown on a flat tantalum

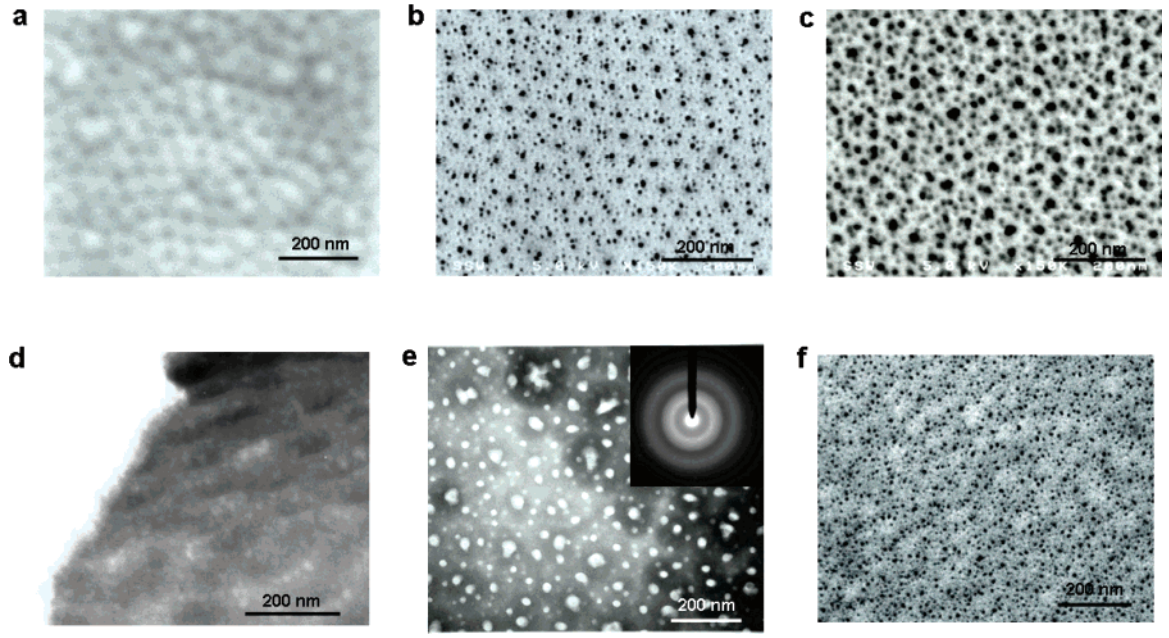

Figure 5. SEM and TEM images of pores in membranes grown under different conditions. (a) SEM image of an oxide film with dimples but no visible pores grown for 5 min in 0.5 wt % HF. (b) SEM image of an oxide film with small pores loosely aligned with dimples grown for 5 min in 2 wt % HF. (c) SEM image of an oxide film with large pores grown for 5 min in 4 wt % HF. (d) TEM image of an oxide film with dimples for 5 min in 0.5 wt % HF. Bright dots are probably due to shallow small pores that were invisible in SEM. (e) TEM image of an oxide film with pores grown for 5 min in 2 wt % HF. Some pores appear to penetrate the membrane. (f) SEM image of an oxide film with small pores grown for 5 min in 2 wt % HF on a previously peeled surface without dimples (such as Figure 3c).

surface (Figure 5f), with larger pores loosely following the dimple pattern. Transmission electron microscopy (TEM) measurements (Figure 5d,e) were also carried on membranes prepared on dimpled tantalum surface by anodization for 5 min in 2 wt % HF/1M H_2SO_4 and 0.5 wt % HF/1M H_2SO_4 solutions at 20 V and transferred on copper grids of mesh size 50. Membranes fabricated in 0.5 wt % HF have very small pores that do not penetrate the dimpled membrane (Figure 5d). On the other hand, the membranes prepared in 2 wt % solution have large diameter pores that penetrate the membrane, whereas smaller size pores terminate before reaching the other end (Figure 5e).

The diffuse electron diffraction pattern of the corresponding TEM image (inset of Figure 5e) indicates that the oxide in the membranes is amorphous. This is confirmed by X-ray diffraction (XRD), the results of which are provided as Supporting Information. The XRD spectra did not show any characteristic peak of the orthorhombic or hexagonal phase of Ta_2O_5, and we could not determine the exact structure of the regular nanocrystalline lattice. However, simulating the spectra using an orthorhombic basis set calculates the crystal size to be around 1.5 nm. For microelectronic applications, the absence of crystallinity in Ta_2O_5 films is expected to be beneficial.[14] Annealing the membranes at around 700 °C under appropriate conditions will lead to crystallization, as has already been demonstrated for anodized tantalum oxide films.[14] Consequently, their mechanical properties and pore size[46] can be further tuned due to volume contraction.

The porosity of these tantalum oxide membranes was calculated by comparing the thickness of the detached oxide membranes on a silicon substrate as measured by atomic force microscopy (AFM) with that of the total amount of oxide measured by NRA (Figure 6b). The oxide membranes grown at 20 V for 1, 2, 5, 8, and 10 min in 2 wt % HF and 1M H_2SO_4 were transferred onto Si (111) wafers, and the step height of the Ta_2O_5 membrane was measured at the edge using AFM (Figure 6a). The porosity of the films increases with the thickness of the oxide layer and ranges from 20 vol % to 45 vol %. The thickness of oxide films increases at an average rate of about 8−9 nm per min. Also, the rate of dissolution increases with time because at the end the remaining oxide grows at a constant rate of 3.8 nm per min (slope of NRA graph).

To better quantify the quality of our tantalum oxide membranes, we carried out refractive index measurements using iterative ellipsometry (Philips PZ-200 with HeNe laser, rotating analyzer) on five different tantalum oxide samples. Ellipsometry on porous films is nontrivial because of possible inhomogeneities of the pores within the film,[47] the presence of adsorbates or humidity inside the pores, or in our case also the presence of F^- and SO_4^- ions inside the oxide. Tantalum substrates were anodized in a 2 wt % HF/1M H_2SO_4 solution at 20 V for 1, 2, 5, 8, and 10 min, respectively, and the resulting films were transferred onto glass slides. The average refractive index obtained by the iterative method for these membranes is 1.98 (±0.02), which is slightly lower than the 2.1 reported for compact tantalum oxide.[48] The high refractive index of these membranes makes them ideal candidates for use in photonic crystals and waveguides. A detailed study is currently underway to further enhance their optical and mechanical properties as well as their surface morphology and pore size by annealing or tailoring electrochemical etching conditions.

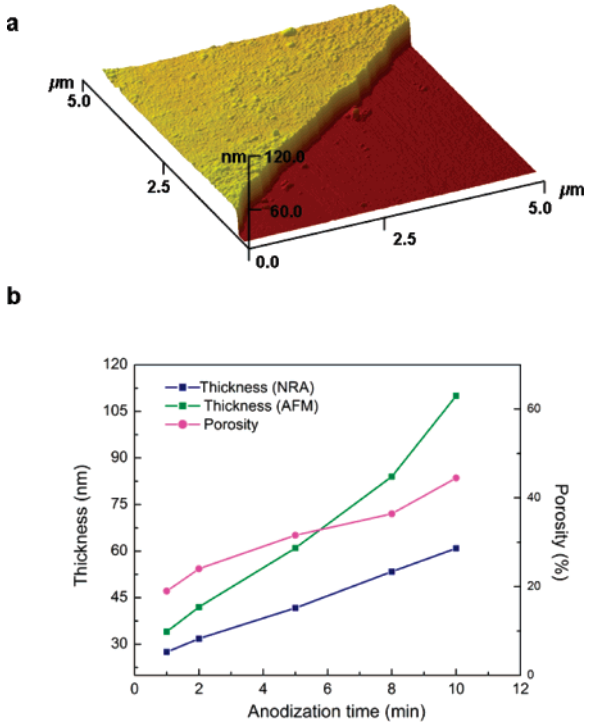

Figure 6. Film thickness and porosity. (a) AFM image of the edge of a tantalum oxide film growth for 5 min and transferred onto silicon, as it was used to measure film thickness. (b) Absolute thickness (T) of the membrane (by AFM), total amount of oxide (O, by NRA), and resulting porosity (P) as a function of anodizing time in 1M H_2SO_4, 2 wt % HF solution at 20 V. The porosity (P) was calculated as $P = (T - O)/T$.

In summary, we have presented a simple and inexpensive way of making self-supporting, extremely thin membranes of pure tantalum oxide with remarkable control over their morphology, thickness, and porosity. The principle behind the fabrication of these membranes is the utilization of differential diffusivity of anions from the electrolyte during the anodization of a metal surface to form a "Sollbruchstelle" (predetermined breaking point) between the oxide layer and the metal. Anions that combine with the metal cations to form the insoluble membrane (e.g., O^{2-}) diffuse more slowly and dominate the outer layer, whereas anions that form the soluble Sollbruchstelle layer (e.g., F^-) quickly diffuse to the oxide layer−metal interface. The key to applying this principle lies in finding the suitable chemical system of solvent (e.g., water), insoluble membrane material (e.g., Ta_2O_5), and soluble Sollbruchstelle (e.g., TaF_5). Our method allows membrane transfer onto virtually any substrate, including biological and other soft materials, by removing the potential for physical damage resulting from most vacuum deposition procedures. On the basis of the exceptional properties of tantalum oxide, these porous membranes will find applications in photocatalysis, molecular filtration membranes, Bragg-like sensors, and dielectric spacers. Furthermore, extension of our work to other metal oxides like niobium, titanium, and hafnium would permit the fabrication of similar high aspect ratio oxide membranes, which are in great demand for catalysts, photovoltaics, and electronic devices.

Acknowledgment. We are grateful to William N. Lennard (Interface Science Western) for help with NRA, James Francis, Luan Xi, and Heng Yong Nie for help with SIMS, Ross Davidson (all Surface Science Western) and Steve Koprich for help with SEM, Fred Pearson for help with TEM, Jim Britten (all Brockhouse Institute for Materials Research) for help with XRD, and Graham Pearson (Centre for Emerging Device Technologies) for assistance with ellipsometry. The work was financially supported by the Natural Science and Engineering Research Council of Canada and an Ontario Premier's Research Excellence Award.

Supporting Information Available: Experimental details and mass spectra for secondary ion mass spectrometry as well as X-ray diffraction data with experimental details. This material is available free of charge via the Internet at http://pubs.acs.org.

References

(1) Wollaston, W. H. On the identity of columbium and tantalum. *Philos. Trans. R. Soc. London* **1809**, *1*, 246−252.
(2) Findlay, D. M.; Welldon, K.; Atkins, G. J.; Howie, D. W.; Zannettino, A. C. W.; Bobyn, D. *Biomaterials* **2004**, *25*, 2215−2227.
(3) Macionczyk, F.; Gerold, B.; Thull, R. *Surf. Coat. Technol.* **2001**, *142*−*144*, 1084−1087.
(4) Christensen, C.; Reus, R.; Siebe, B. *J. Micromech. Microeng.* **1999**, *9*, 113−118.
(5) Sreethawong, T.; Ngamsinlapasathian, S.; Suzuki, Y.; Yoshikawa, S. *J. Mol. Catal. A: Chem.* **2005**, *235*, 1−11.
(6) Zou, Z.; Ye, J.; Sayama, K.; Arakawa, H. *Nature* **2001**, *414*, 625−627.
(7) Rubio, J.; Denis, J. M.; Albella, J.; Martinez-Duart, M. *Thin Solid Films* **1982**, *90*, 405−408.
(8) Nakagawa, Y.; Yawata, M.; Kakio, S. Enhancement of photoelasticity assisted by surface acoustic wave and its application to the optical modulator. *Electron. Commun. Jpn., Part II: Electron.* **2001**, *84*, 46−54.
(9) Alers, G. B.; Werder, D. J.; Chabal, Y.; Lu, H. C.; Gusev, E. P.; Garfunkel, E.; Gustafsson, T.; Urdahl, R. S. *Appl. Phys. Lett.* **1998**, *73*, 1517−1519.
(10) Ueno, K.; Abe, S.; Onoki, R.; Saiki, K. *J. Appl. Phys.* **2005**, *98*, 114503.
(11) Teravaninthorn, U.; Miyahara, Y.; Moriizumi, T. *Jpn. J. Appl. Phys.* **1987**, *26*, 2116−2120.
(12) Kingon, A. I.; Maria, J. P.; Streiffer, S. K. *Nature* **2000**, *406*, 1032−1038.
(13) Devine, R. A. B.; Chaneliere, C.; Autran, J. L.; Balland, B.; Paillet, P.; Leray, J. L. *Microelectron. Eng.* **1997**, *36*, 61.
(14) Chaneliere, C.; Autran, J. L.; Devine, R. A. B.; Balland, B. *Mater. Sci. Eng.* **1998**, *R22*, 269−322.
(15) Zhang, S.; Fan, W.; Panoiu, N. C.; Malloy, K. J.; Osgood, R. M.; Brueck, S. R. J. *Phys. Rev. Lett.* **2005**, *95*, 137404.
(16) Shalaev, V. M.; Cai, W.; Chettiar, U. K.; Yuan, H.-K.; Sarychev, A. K.; Drachev, V. P.; Kildishev, A. V. *Opt. Lett.* **2005**, *30*, 3356−3358.
(17) Lu, Q.; Mato, S.; Skeldon, P.; Thompson, G. E.; Masheder, D.; Habazaki, H.; Shimizu, K. *Electrochim. Acta.* **2002**, *47*, 2761−2767.
(18) Young, L. *Proc. R. Soc. London, Ser. A* **1960**, *258*, 496−515.
(19) Sieber, I.; Schmuki, P. *J. Electrochem. Soc.* ***2005***, *152*, C639−C644.
(20) Vermilyea, D. A. *Acta Metall.* **1954**, *2*, 483−486.
(21) Shimizu, K.; Brown, G. M.; Habazaki, H.; Kobayashi, K.; Skeldon, P.; Thompson, G. E.; Wood, G. C. *Corros. Sci.* **1998**, *40*, 963−973.
(22) Sayed, H. E.; Singh, S.; Greiner, M. T.; Kruse, P. *Nano Lett.* **2006**, *6*, 2995−2999.
(23) Sakai, H.; Furukawa, Y.; Fujiwara, E.; Tada, H. *Chem. Lett.* **2004**, *33*, 1172−1173.
(24) Demiryont, H.; Sites, J. R.; Geib, K. *Appl. Opt.* **1985**, *24*, 490−495.
(25) Waldorf, A. J.; Dobrowolski, J. A.; Sullivan, B. T.; Plante, L. M. *Appl. Opt.* **1993**, *32*, 5583−5593.
(26) Zaima, S.; Furuta, T.; Yasuda, Y.; Iida, M. *J. Electrochem. Soc.* **1990**, *137*, 1297−1300.

(27) Lo, G. Q.; Kwong, D. L.; Lee, S. *Appl. Phys. Lett.* **1992**, *60*, 3286−3288.
(28) Pollard, K. D.; Puddephatt, R. J. *Chem. Mater.* **1999**, *11*, 1069−1074.
(29) Gu, G.; Schmid, M.; Chiu, P.-W.; Minett, A.; Fraysse, J.; Kim, G.-T.; Roth, S.; Kozlov, M.; Muñoz, E.; Baughman, R. H. *Nat. Mater.* **2003**, *2*, 316−319.
(30) Yang, H.; Coombs, N.; Sokolov, I.; Ozin, G. A. *Nature* **1996**, *381*, 589−592.
(31) Vendamme, R.; Onoue, S. Y.; Nakao, A.; Kunitake, T. *Nat. Mater.* **2006**, 5, 494−501.
(32) Wang, X.; Lao, C.; Graugnard, E.; Summers, C. J.; Wang, Z. L. *Nano Lett.* **2005**, *5*, 1784−1788.
(33) Choi, S. Y.; Mamak, M.; Freymann, G. V.; Chopra, N.; Ozin, G. A. *Nano Lett.* **2006**, *6*, 2456−2461.
(34) Pan. S.; Rothberg, L. J. *Nano Lett.* **2003**, *3*, 811−814.
(35) Lin, V. S. Y.; Motesharei, K.; Dancil, K. S.; Sailor, M. J.; Ghadiri, M. R. *Science* **1997**, *278*, 840−843.
(36) Potyrailo, R. A.; Ghiradella, H.; Vertiatchikh, A.; Dovidenko, K.; Cournoyer, J. R.; Olson, E. *Nat. Photonics* **2007**, *1*, 123−129.
(37) Davies, J. A.; Norton, P. R. *Nucl. Instrum. Methods* **1980**, *168*, 611−615.
(38) Shimizu, K.; Kobayashi, K.; Thompson, G. E.; Skeldon, P.; Wood, G. C. *Philos. Mag. B* **1996**, *73*, 461−485.
(39) Shimizu, K.; Kobayashi, K.; Thompson, G. E.; Skeldon, P.; Wood, G. C. *J. Electrochem. Soc.* **1997**, *144*, 418−423.
(40) Lide, D. R. *CRC Handbook of Chemistry and Physics*, 72th Ed.; CRC Press: Boca Raton, FL, 1991.
(41) Vilan, A.; Cahen, D. *Adv. Funct. Mater.* **2002**, *12*, 795−807.
(42) Alcala, G.; Skeldon, P.; Thompson, G. E.; Mann, A. B.; Habazaki, H.; Shimizu, K. *Nanotechnology* **2002**, *13*, 451−455.
(43) Rizkalla, H.; Wellinghoff, S. T. *J. Mater. Sci.* **1984**, *19*, 3895−3907.
(44) Masuda, H.; Fukuda, K. *Science* **1995**, *268*, 1466−1468.
(45) Yamaguchi, A.; Uejo, F.; Yoda, T.; Uchida, T.; Tanamura, Y.; Yamashita, T.; Teramae, N. *Nat. Mater.* **2004**, *3*, 337−341.
(46) Striemer, C. C.; Gaborski, T. R.; McGrath, J. L.; Fauchet, P. M. *Nature* **2007**, *445*, 749−753.
(47) Herrero, A. A.; Guerrero, H.; Bernabeu, E.; Levy, D. *Appl. Opt.* **2002**, *41*, 6692−6701.
(48) Ezhilvalavan, S.; Tseng, T. Y. *J. Mater. Sci.: Mater. Electron.* **1999**, *10*, 9−31.

NL071061Z